FAR-FIELD S-WAVE SPECTRA, CORNER FREQUENCIES, AND PULSE SHAPES

James N. Brune, Ralph J. Archuleta,[1] and Stephen Hartzell

Institute of Geophysics and Planetary Physics, Scripps Institution of Oceanography
La Jolla, California 92093

Abstract. Recent results concerning the relationship of S-wave far-field corner frequencies to stress drop are discussed. It is suggested that the corner frequency as picked by Madariaga [1977] from his theoretical spectra is not consistent with the way in which corner frequencies were picked by Tucker and Brune [1973, 1977]. When the difference is taken into account, the stress drops inferred from the Madariaga relationship and his method of picking corner frequencies are roughly the same as inferred using the Brune [1970, 1971] relationship and the Tucker and Brune method of picking corner frequencies (for those relatively few experimental spectra which are similar in shape to the Madariaga theoretical spectra). Far-field spectra for a number of new finite element models of fault ruptures in a half-space are presented, and for these data, new values for the relationship between source dimension and corner frequency are obtained. Fault models used include semicircular faults with rupture initiation at the surface and at depth and rectangular faults with unilateral and bilateral rupture propagation. The results indicate that there is a considerable variation in corner frequency with respect to type of rupture and position around the rupture. Because of the variation it is not possible to conclude, without more calculations, what the best average relationship between corner frequency and source dimension is; however, a value of K about 1/3 is reasonable where $K = f_c r/\beta$ (f_c = corner frequency, r = radius, and β = shear wave velocity). Dahlen [1974] speculated that the corner frequencies picked experimentally could be significantly altered by scattering. For the San Fernando aftershocks, it is possible to make a case that this is not so. Many of the San Fernando aftershocks show very simple pulse shapes, with a pulse duration consistent with the spectral corner frequency and little later arriving energy - a direct indication that scattering is not radically affecting the results.

Introduction

Studies of far-field spectra and pulse shapes of earthquakes offer the possibility of estimating the level and variability of tectonic stress. This possibility is especially attractive if small earthquakes can be used, since they occur so frequently. However, testing the reliability and usefulness of such studies and comparing the results with results obtained from larger earthquakes using aftershock distributions and surface breaks will require more experimental and theoretical work. We need reliable near-field recordings at a large number of observation points on the focal sphere of earthquakes to obtain accurate information about source parameters such as dimension, rupture velocity, and stress drop. For comparison with theory, we need to examine more fault models to determine the effects of stress drop, friction, and rupture velocity on spectra and pulse shapes. In this paper we present some further discussion of the experimental digital data obtained from aftershocks of the San Fernando earthquake and the theoretical data obtained from finite element numerical models of earthquake rupture.

San Fernando Aftershock Data

The main experimental data discussed in this paper is the data obtained by Tucker and Brune [1973, 1977] from aftershocks of the San Fernando earthquake. In those studies, high-dynamic range, broadband digital data were used to determine near source earthquake spectra. These were then interpreted to infer seismic moment, source dimension, and stress drop using formulas given by Brune [1970, 1971]. The results suggested a wide range in stress drops, with an upper limit of about 200 bars, and many cases of stress drop less than 1 bar. A number of the larger events (M = 3.5-4) apparently had two corner frequencies, one between 0.1 and 1 Hz, below which the spectra were approximately constant, and another between 3 and 10 Hz, above which spectra were proportional to about ω^{-2} to ω^{-3}. It was suggested that for these larger events with two corner frequencies, a two-stage rupture process may have occurred, an initial sharp high stress drop followed by a more slowly growing rupture. Similar results were found by Hartzell and Brune [1977] for earthquakes occurring in the Brawley swarm of January 1975. We will not discuss these results further in this paper but will use the experimental data to investigate the method of determining corner frequencies and the relationship of corner frequency to source dimension and hence stress drop. All the experimental seismograms and spectra are taken from Tucker and Brune [1973] using their numbering. The horizontal arrow under each seismogram indicates the time window for the Fourier transform used to obtain the spectra (Figures 2-4).

Madariaga's Theoretical Model Results

Madariaga [1976, 1977] used a numerical finite difference method to compute the dislocation rate on a growing circular fault which stopped at a certain radius r (in a full space). With the slip velocity and the far-field representation

[1]U. S. Geological Survey, 345 Middlefield Road, Menlo Park, California 94025

Paper number 8B0925.
0148-0227/79/058B-0925$01.00

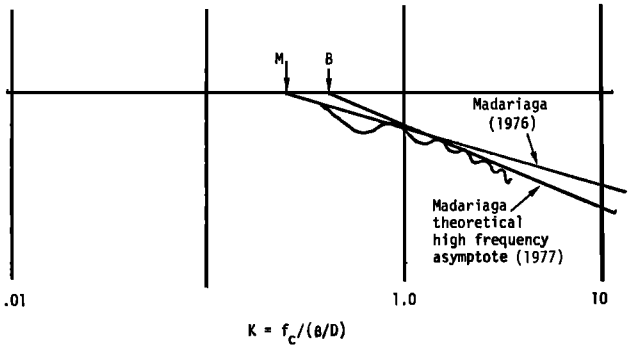

Fig. 1. Theoretical far-field spectrum of Madariaga at an angle of 60° from the normal to a circular fault in a full space. The two high-frequency asymptotes define two corner frequencies, M and B. The corner frequency marked B yields a K value very close to the K value for the Brune model.

integral, Madariaga computed the far-field spectra at different azimuths. For these results he obtained an average spectrum for a rupture velocity of 0.9β at an angle of 60° from the normal to the fault (Figure 1). For this spectrum, he drew a low-frequency asymptote and a higher-frequency asymptote to determine the corner frequency f_c (indicated by M in Figure 1). From f_c he determined $K = f_c r/\beta = 0.21$, where r is the fault radius and β the shear wave velocity. This value of K is considerably lower than the value of K for the Brune model, $K = 0.37$. Since the formula for determining stress drop from corner frequency depends on the third power of corner frequency, Madariaga's relationship implies a stress drop 5.47 times higher than Brune's. This would mean that for the San Fernando aftershocks the estimated upper bound on stress drops would be closer to 1 kbar than to 200 bars as inferred by Tucker and Brune. Since the values of stress drop determined from earthquakes have played a considerable role in recent discussions about earthquake source mechanisms, this uncertainty is important, and hence we wish to investigate further the interpretation of earthquake corner frequencies.

In a second paper, Madariaga [1977] also calculated a high-frequency asymptote which, if used to infer corner frequency, gave a value for K of 0.40 (indicated by B in Figure 1). If this

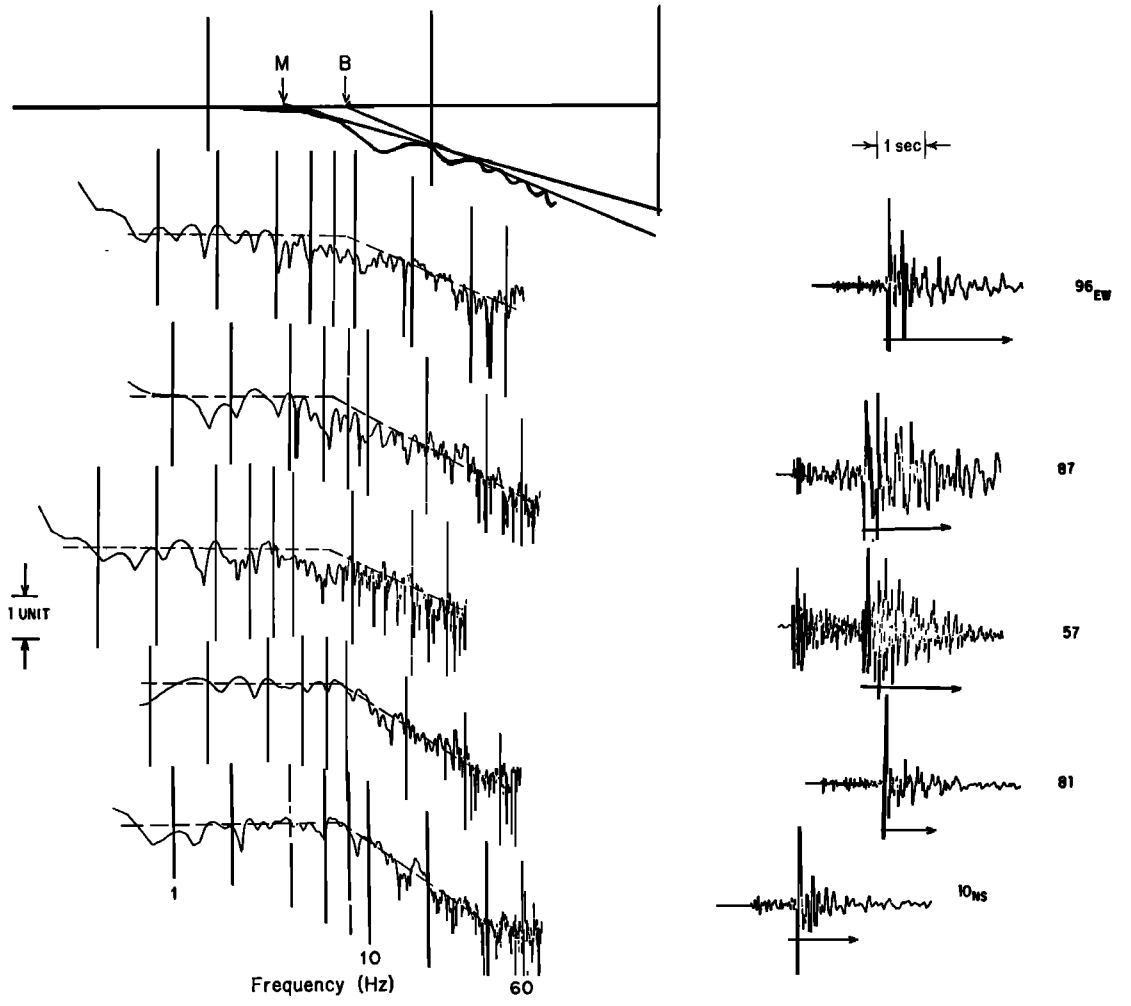

Fig. 2. Comparison between the theoretical Madariaga spectrum (top, taken from Figure 1) and a number of the Tucker and Brune spectra for aftershocks of the San Fernando earthquake plotted on the same scale. Spectra have been adjusted horizontally to line up spectral corners.

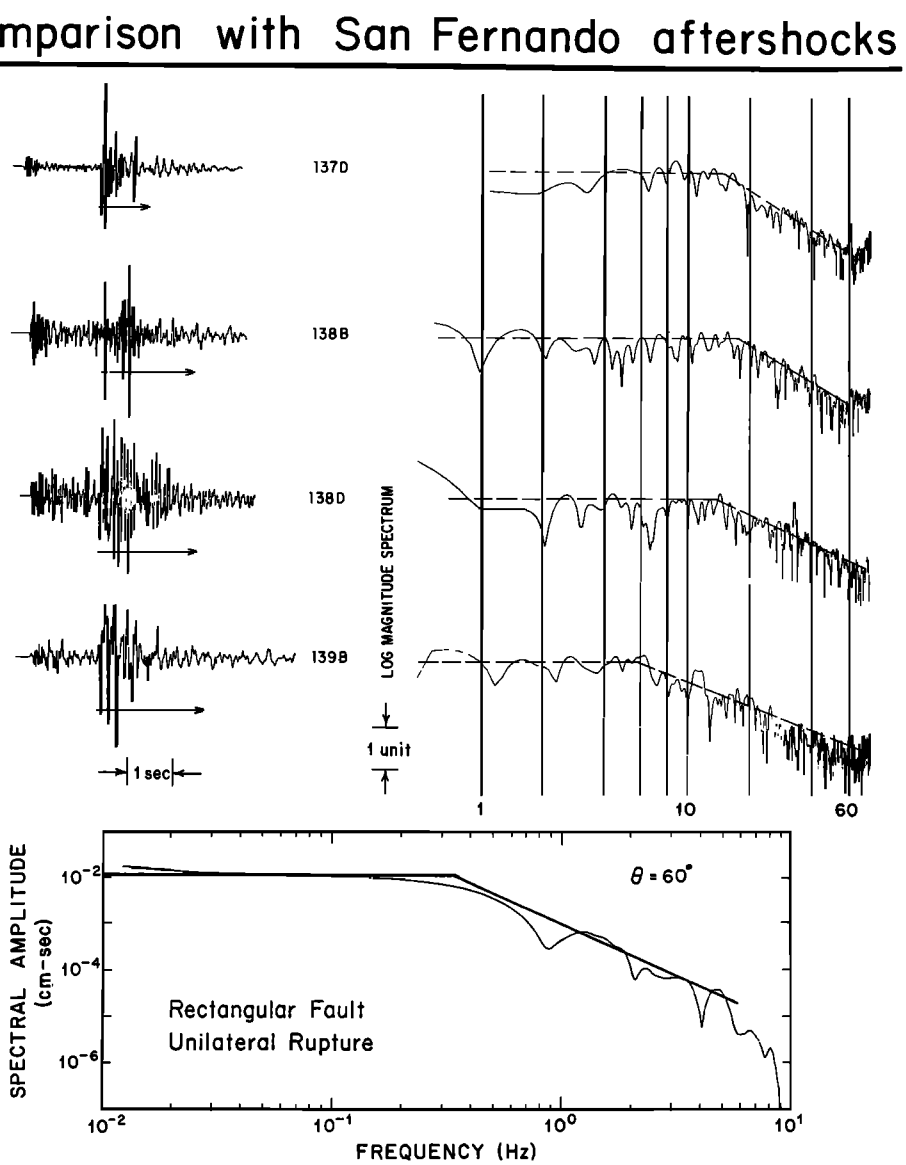

Fig. 3. Comparison between the far-field spectrum at 60° for a rectangular fault, aspect ratio of 5 and unilateral rupture propagation, with selected spectra of San Fernando aftershocks.

value of K were used, nearly the same values of stress drop as found by Tucker and Brune would be obtained.

It appears that the method of picking corner frequencies and, in particular, the weight put on high frequencies, is important. This is particularly true in the case of numerical modeling, since it is difficult and costly to adequately represent frequencies much above a factor of 2 or 3 times the corner frequency. This is why Madariaga had to use other techniques to estimate the higher-frequency asymptote. At this point it is necessary to decide whether the method of picking corner frequencies used by Madariaga is consistent with that used by Tucker and Brune.

Comparison of the Tucker and Brune Experimental Spectra with the Madariaga Theoretical Spectra

In order to compare the theoretical and experimental spectra, we have plotted the Madariaga spectrum and a number of Tucker and Brune spectra on the same scale (Figure 2). Comparison with the more than 100 spectra presented by Tucker and Brune shows that one of the characteristics of the Madariaga spectrum is a more flattened corner than observed for most of the Tucker and Brune spectra. Figure 2 was purposely selected to show examples of some of the Tucker and Brune spectra which have this character, i.e., a flattened corner or missing energy near the corner frequency (top three spectra in Figure 2). Most of the Tucker and Brune spectra have sharper corners, like the bottom two examples in Figure 2, and hence there is little uncertainty in determining a corner frequency. Because of the difference in shape between the Madariaga spectrum and most of the Tucker and Brune spectra, there is some doubt about the growing and stopping circular crack as a model for the San Fernando aftershocks.

The dashed lines in Figure 2 show the asymptotes used to infer corner frequencies by

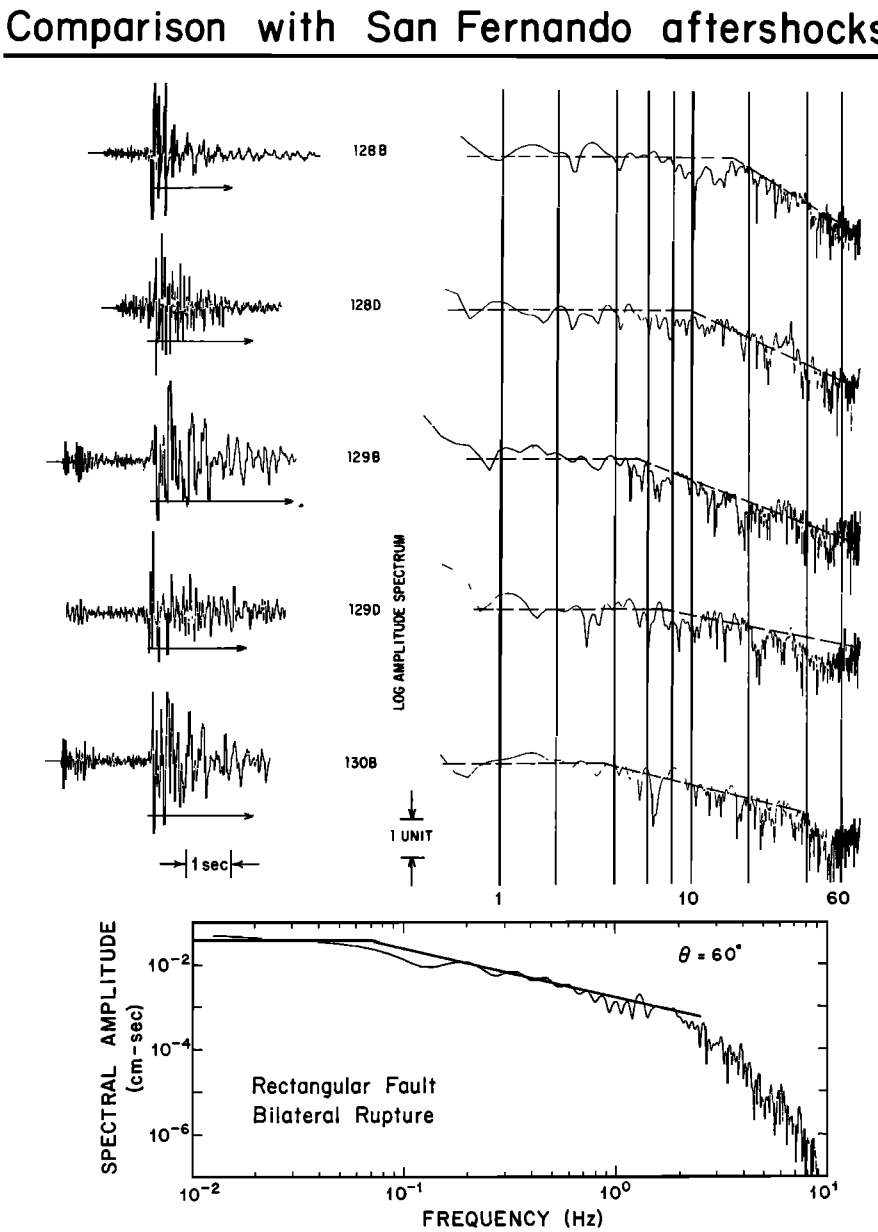

Fig. 4. Comparison between the far-field spectrum at 60° for a rectangular fault, aspect ratio of 4 and bilateral rupture propagation, with selected spectra of San Fernando aftershocks.

Tucker and Brune, and these can be compared with the asymptotes used by Madariaga to interpret the theoretical spectra as shown in the upper part of Figure 2. It is immediately obvious that the corner frequency picked by Madariaga, indicated by an M in the upper theoretical spectrum, is considerably lower than would have been picked by Tucker and Brune, whereas the corner frequency determined from the high-frequency asymptote of Madariaga, indicated by B, corresponds nearly exactly with the corner frequency as determined by Tucker and Brune.

Since the Madariaga high-frequency asymptote gives a corner frequency to fault radius relationship almost identical to that used by Tucker and Brune (K = 0.40 versus K = 0.37), it is evident that the interpretation of stress drops by Tucker and Brune is in accordance with the theoretical spectra of Madariaga. The further question of why the shape of most of the Tucker and Brune spectra are different from the shape of the Madariaga spectra is left unanswered. Some recent results pertinent to this are discussed in the next section.

New Results for Far-Field Pulse Shapes and Spectra Based on Finite Element Models of Fault Rupture

Archuleta and Frazier [1978] have presented results for finite element models of faulting based on stress relaxation. The resulting time functions for fault slip at various points on the fault can be used to compute the far-field radiation. Half space Green's functions, computed using a program of Johnson [1974], for each point on the fault surface, are convolved with the slip functions on the fault and summed

to give the complete far-field pulse [Hartzell *et al.*, 1978, Hartzell, 1978].

The following are the far-field SH pulses observed on the surface of an elastic half space for four different fault models: (1) a semicircular fault in which rupture initiation begins at the surface (r = 0) and propagates radially to a specified fault radius, with 10 elements on a radius, (2) a semicircular fault in which rupture initiation begins at the deepest point on the fault and symmetrically propagates over the semicircle, breaking out at the surface, also with 10 elements on a radius, (3) a rectangular fault 3 elements deep and 15 elements long in which rupture propagation proceeds unilaterally from one end to the other, and (4) a rectangular fault 5 elements deep and 20 elements long in which rupture proceeds bilaterally from the center to both ends.

A rupture velocity of 0.9β is used for each of the four fault models above. Results for the far-field time functions (azimuthal component) are shown in Figures 5a and 5b, and the corresponding spectra (S phase only) at the bottom of Figures 3 and 4 and in Figures 6 through 9. All of the numerical results shown here are for surface observations, with the azimuthal angle relative to the normal to the fault as a

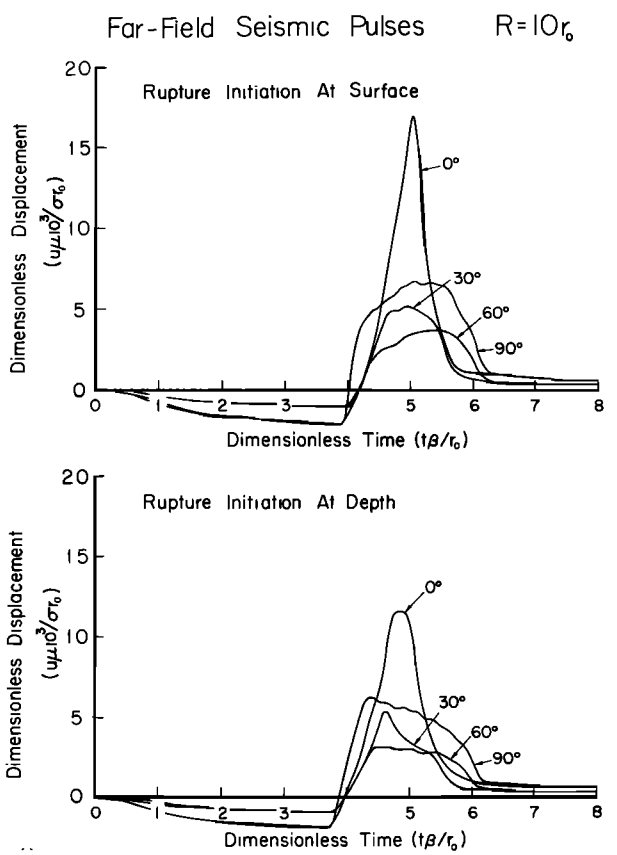

Fig. 5a. Far-field surface displacements, transverse component, for two semicircular faults in a homogeneous half space. Displacements are calculated by convolving the slip velocities on the fault from a numerical stress relaxation problem with the Green's functions for a half space. The azimuth of each trace is measured from the normal to the fault.

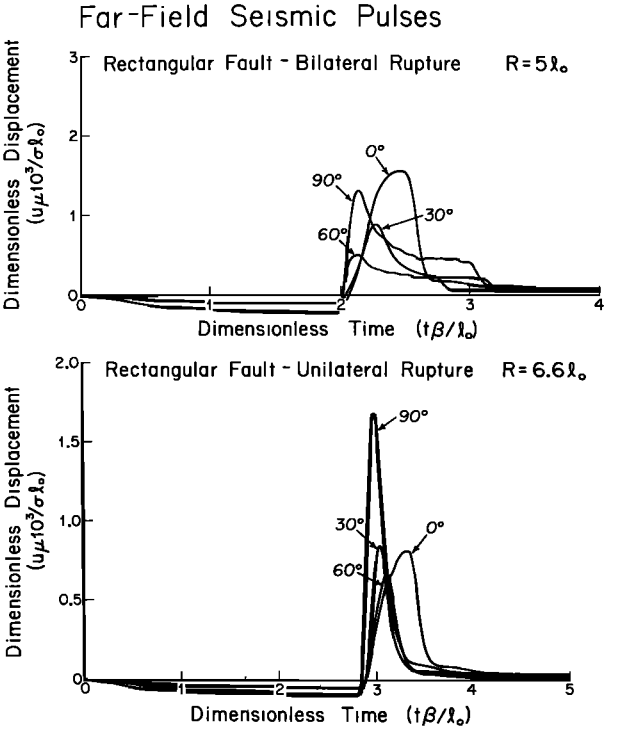

Fig. 5b. Far-field surface displacements, transverse component, for two rectangular faults in a homogeneous half space. Method of calculation is the same as in Figure 5a.

variable. Interpreted corner frequencies are indicated by the intersecting asymptotes drawn on the spectra.

For each fault model, the points of observation are at a constant radial distance R from the center of the fault. R is equal to $10r_o$ for both semicircular faults, $5\ell_o$ for the bilateral rupture, and $6.6\ell_o$ for the unilateral rupture. Here r_o is the radius of the semicircular faults, and ℓ_o is the length of the corresponding rectangular fault. The azimuth of the point of observation is measured from the normal to the fault. In the case of the rectangular unilateral rupture, the time function at 90° is in the direction of rupture propagation. The far-field time functions are plotted in dimensionless format (Figures 5a and 5b), where the dimensionless displacement is given by $u\mu 10^3/\sigma r_o$ for the semicircular faults and $u\mu 10^3/\sigma \ell_o$ for the rectangular faults. Here u is the displacement, μ the rigidity, and σ the effective stress.

Because of the finite grid size, frequencies greater than 2 Hz are not accurately synthesized [Archuleta and Frazier, 1978], and this must be taken into account in interpreting corner frequencies and pulse shapes. Archuleta and Frazier [1978] have shown that their results have somewhat better frequency range than the results of Madariaga. In most cases the frequency range was sufficient to establish the true corner frequency with confidence. To assure objectivity in picking corner frequencies, both Brune and Archuleta independently picked the corner frequencies without knowledge of the other's picks. In nearly all cases the picked corner frequencies agreed within 20%. Since Brune was

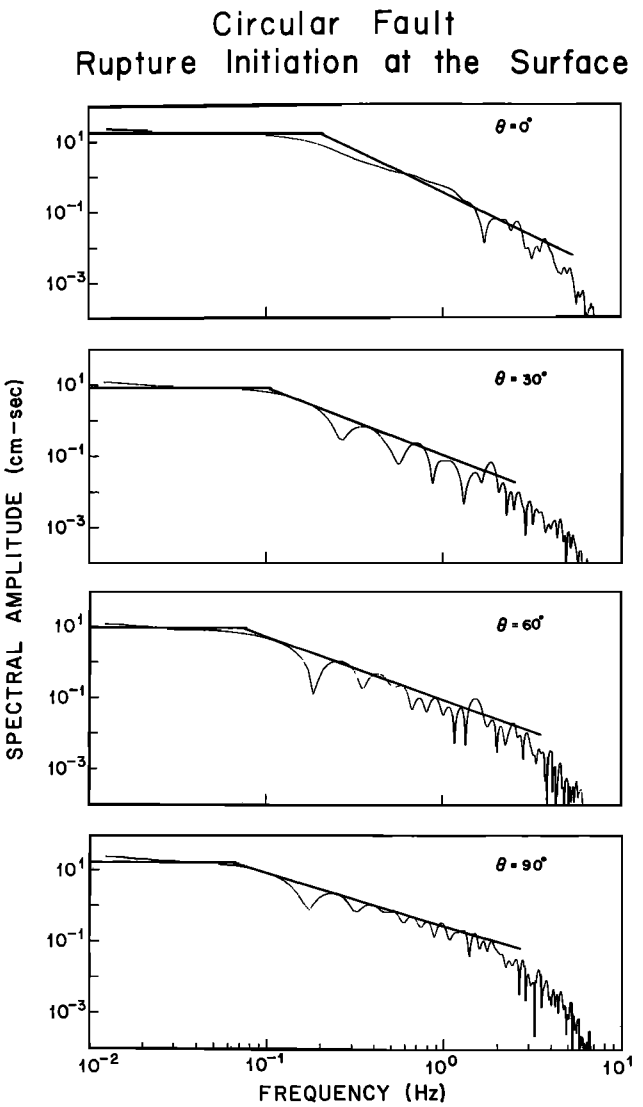

Fig. 6. Displacement amplitude spectra for the far-field seismic pulses pictured at the top of Figure 5a. The azimuth θ is measured from the normal to the fault. The intersections of the indicated low and high frequency asymptotes were used to define the corner frequencies, which in turn yield the K values plotted in Figure 10.

one of the investigators picking corner frequencies in the Tucker and Brune experimental study, there is some assurance that corner frequencies determined there were determined in the same manner as in this study. As a comparison with observed spectra, some of the results for the rectangular faults are shown along with representative spectra of San Fernando aftershocks, chosen to show similar features, in Figures 3 and 4.

Study of the time functions and spectra shows a range of pulse durations and a corresponding range of corner frequencies (inverse proportionality) depending primarily on the azimuth between the direction of rupture propagation and the direction of observation. For bilateral ruptures, the pulse widths are narrower normal to the fault than they are in the direction of rupture; however, the rise times are shorter in the direction of rupture propagation than they are normal to the fault. The pulse width is controlled primarily by the difference in travel times from different points on the fault surface. The rise time is related to focusing caused by directivity and an increase in the slip velocity in the direction of rupture propagation. In the propagating stress relaxation models of Archuleta and Frazier [1978] the slip velocity increases in amplitude in the direction of propagation. Thus, in addition to the common directivity effect [Ben-Menahem, 1961] due to a moving source, we have the effect of increasing slip velocity in the direction of rupture. The combined effect is strong focusing of energy in the direction of rupture propagation. It is this combined effect which leads to the shorter rise times in the direction of rupture propagation. This focusing has also been observed in a laboratory model of propagating stress relaxation [Archuleta and Brune, 1975; Archuleta, 1976, Hartzell, 1978]. For unilateral ruptures, both the pulse width and the rise time decrease as one moves from normal to the fault to in line with the direction of rupture

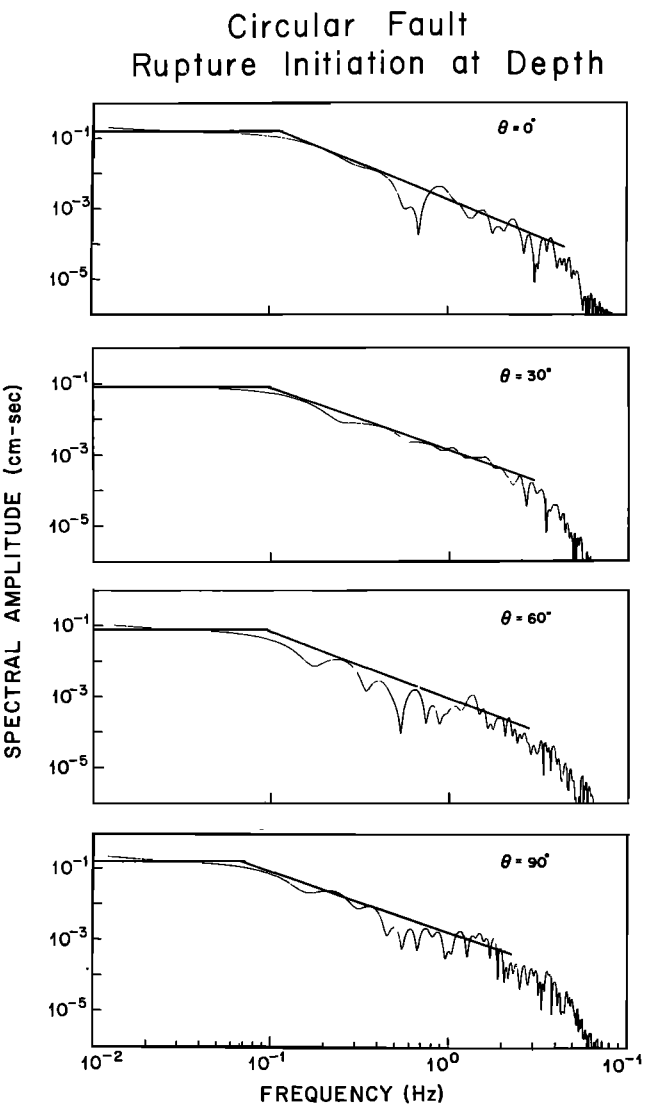

Fig. 7. Displacement amplitude spectra for the far-field seismic pulses pictured at the bottom of Figure 5a. Details are same as Figure 6.

propagation. Short rise times and narrow pulse widths increase the high-frequency content and yield higher corner frequencies and larger values of K. In the direction away from the rupture propagation, for a unilateral rupture, both the pulse width and the rise time are greater, leading to lower values of K. In Figure 10 we show the value of $K = f_c D/\beta$ as a function of azimuth for our fault models and those of Savage and Madariaga. We have also reinterpreted the corner frequencies for the Madariaga spectra using the considerations outlined in the first part of this paper, and these are shown as M in Figure 10. This figure can be used as an aid in interpreting experimental data.

Since for a given fault the corner frequency and, consequently, the relationship between corner frequency and source dimension, are strong functions of azimuth, or position on the focal sphere, it is desirable to know the fault orientation and direction of rupture propagation before interpreting the spectra and time functions in terms of fault parameters such as

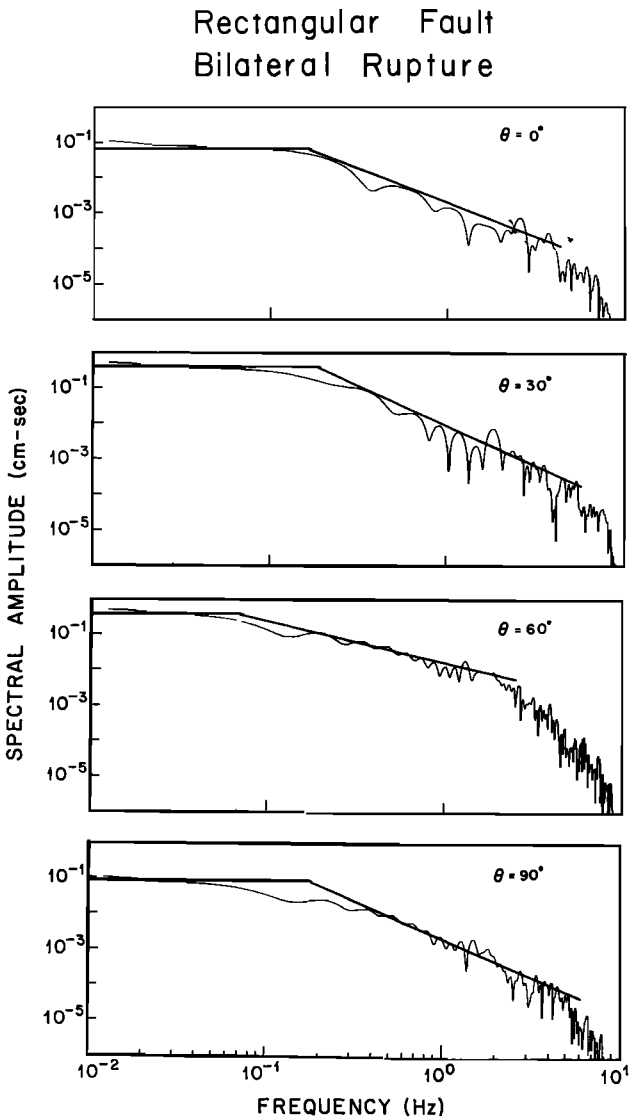

Fig. 8. Displacement amplitude spectra for the far-field seismic pulses pictured at the top of Figure 5b. Details are same as Figure 6.

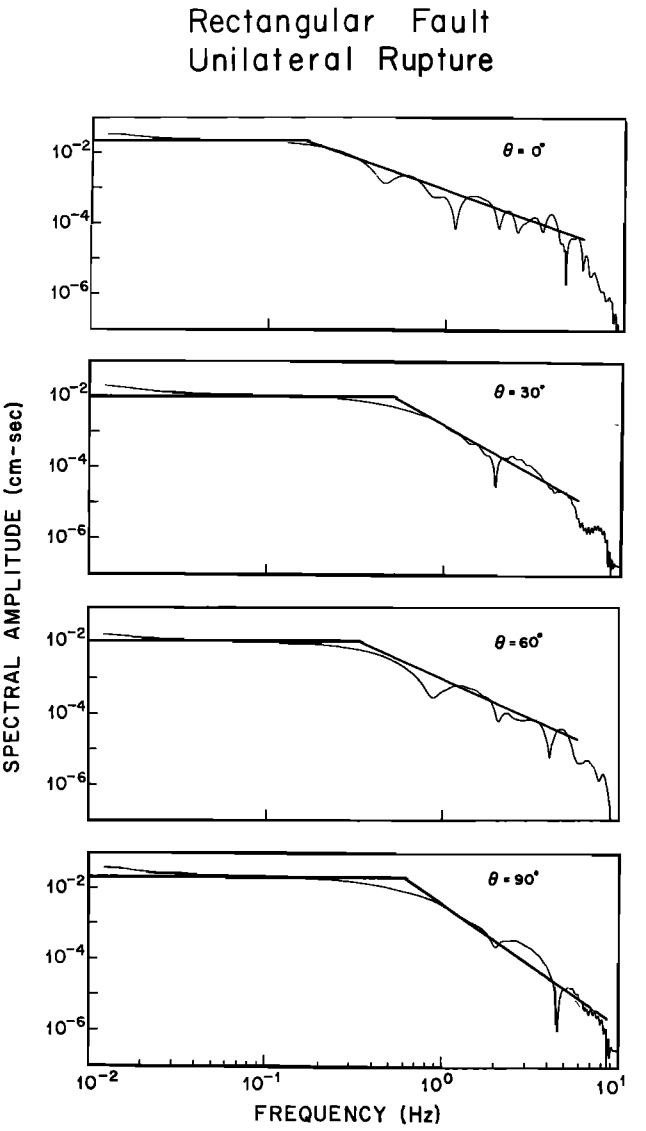

Fig. 9. Displacement amplitude spectra for the far-field seismic pulses pictured at the bottom of Figure 5b. Details are same as Figure 6.

fault dimension, moment, and stress drop. However, in many cases, especially for small earthquakes, this is not possible, and hence it is helpful to have some approximate relationship between corner frequency and fault dimension. Besides Brune and Madariaga, Savage [1972, 1974], Randall [1973], and Dahlen [1974] have also obtained such relationships. To summarize the results of various models, we have shown in Table 1 the values of K for $\theta = 60°$, or in some cases, average values. The value of $\theta = 60°$ was selected by Madariaga because it represents the angle which divides the focal sphere roughly in half (equal areas). Thus, for numerous random observations around the fault, approximately half of the observations should have higher corner frequencies. The value of K for $\theta = 60°$ should not be equated with the corner frequency averaged over the focal sphere, nor should it be equated with the value of K obtained by Brune [1970, 1971], which corresponds to the corner frequency for a spectrum which, if constant over the fault sphere, would, at high frequencies,

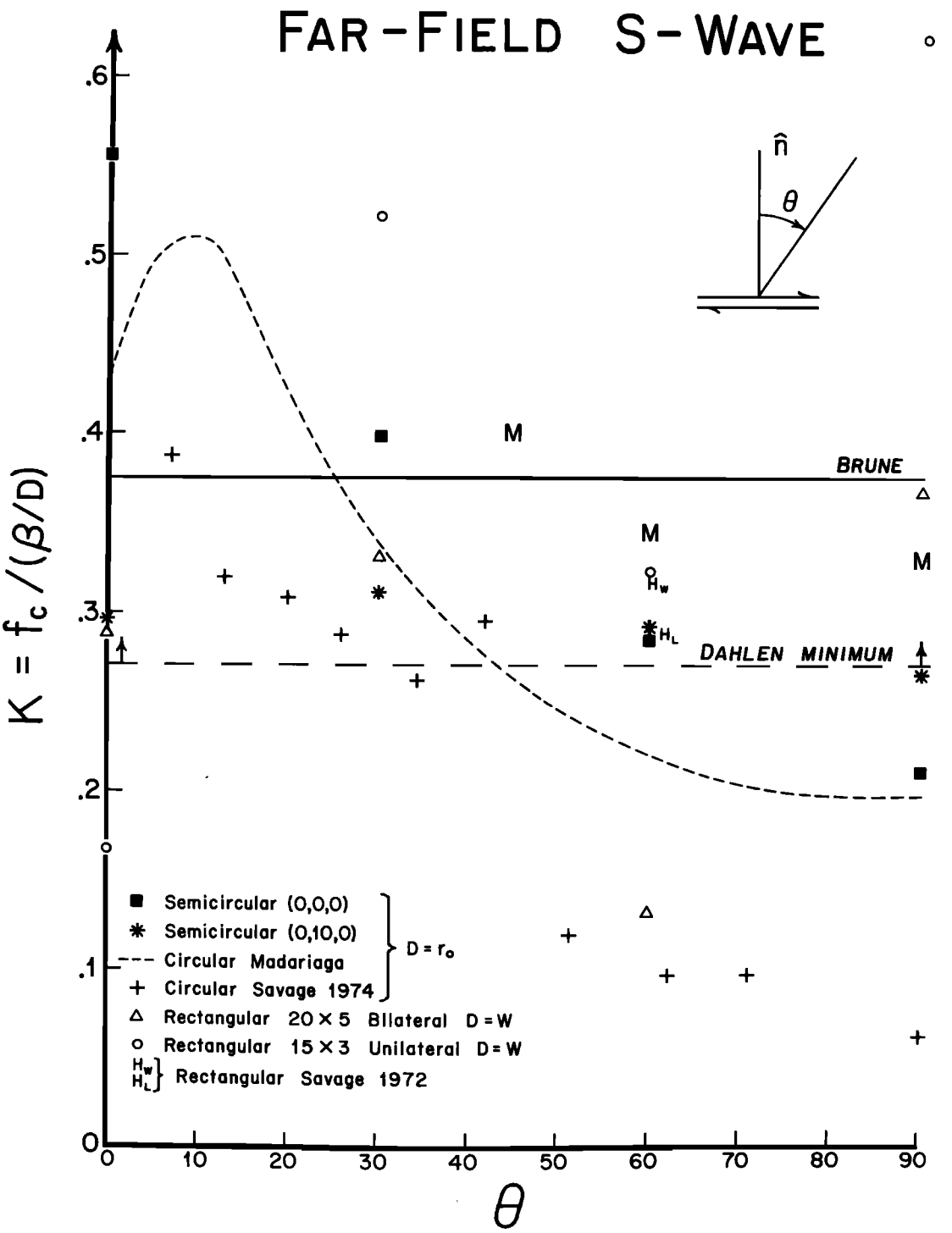

Fig. 10. Summary of the variation in K values with azimuth for far-field S-waves from this study and from other authors. The azimuth θ is measured from the normal to the fault. The rupture velocity is 0.9β for all models, except the Brune model, which is an instantaneous rupture, and the Dahlen minimum line, which corresponds to a rupture velocity equal to β. An M is used to indicate the reinterpreted corner frequency for the Madariaga spectra, chosen consistently with the Tucker and Brune method of picking corner frequencies.

give the same total energy radiation as the actual variable spectrum. However, the values of K determined in the various ways should be roughly comparable. The values for K in Table 1 range from 0.13 to 0.49. The low value of 0.13 corresponds to a bilateral rupture, and the corresponding spectrum (Figure 4, bottom) has a broad intermediate slope proportional approximately to ω^{-1}. At other azimuths the bilateral rupture produces values of K near 0.3, Figure 10. This spectrum is quite different from most of the other spectra and from most of the spectra observed by Tucker and Brune. However, some of the Tucker and Brune spectra did show such a

TABLE 1. K Values (= $f_c/(\beta/D)$) for Far-Field S-Wave, $\theta = 60°$, $v = 0.9\beta$

Source	K Value
Semicircular Faults in a Half Space, $D = r_o$	
This study	
Origin (0, 0, 0)	0.26
Origin (0, r_o, 0)	0.29
Rectangular Faults, D = W	
This study: half space	
L = 4W bilateral	0.13
L = 5W unilateral	0.32
Savage [1972, 1974] (Haskell [1964]): full space	
$L \simeq W$ bilateral	0.32
L >> W bilateral	0.29
Circular Faults in a Full Space, $D = r_o$	
Madariaga [1976, 1977]	
Finite difference spectrum	0.21
High-frequency asymptote	0.40
Dahlen [1974]	0.45
Brune [1970, 1971] ($v = \infty$)	0.37*
Randall [1973]; Archambeau [1968] ($v = \infty$)	0.42*
Dislocation Models	
Molnar *et al.* [1973] ($\theta = 55°$)	0.32
Savage [1972, 1974]	0.49 (0.1)

* Average values

broad ω^{-1} region and as would be expected gave low stress drops when interpreted using a K value of 0.37. Considering the rest of the results, this low value can be considered to a certain extent anomalous.

Although the results of Table 1 are derived from a variety of different earthquake models, an average value of K for ruptures with $v = 0.9\beta$ is 0.32. If the models of Brune [1970, 1971] and Randall [1973] ($v = \beta$) are included, then K becomes 0.33. In view of the many uncertainties in relating theoretical models to actual earthquakes, a reasonable average value of K is 1/3. It must be noted that for a given station recording an earthquake, K could possibly range between 0.15 and 0.5, i.e., $K = 1/3 \pm (0.5)(1/3)$. A 50% error in K corresponds to an error in inferred stress drops of a factor of 3.3. This factor is consistent with the variation in stress drops computed by Tucker and Brune between two different stations for the San Fernando aftershocks.

Scattering and Corner Frequency

Dahlen [1974], observing that the ratio of corner frequencies of P-waves and S-waves observed by Molnar *et al.* [1973] was inconsistent with a source mechanism theory he had developed, suggested that the observed corner frequencies may have been seriously perturbed by scattering. A small amount of scattered energy arriving slightly after the S-wave would not cause a frequency shift in the spectrum, since the reflected pulses would have nearly the same spectrum as the direct energy. The existence of a certain amount of scattering is one of the main reasons for using the spectrum rather than the direct time function - the time function can be seriously distorted by scattering without seriously affecting the amplitude spectrum (which is based on the modulus of the Fourier transform and not the phase). In order for scattering to affect the corner frequencies seriously, a significant fraction of the energy would have to be scattered to travel paths that cause the scattered energy to arrive considerably later than the main energy. This would imply that the S-wave pulse would be considerably distorted or complicated. Thus, in a qualitative way we can estimate the importance of scattering by looking at pulse shapes. A large number of seismograms of aftershocks of the San Fernando earthquake published by Tucker and Brune [1973] can be used for this purpose.

Perusal of the seismograms of the San Fernando aftershocks immediately reveals a wide range of apparent pulse shapes, ranging from simple pulses of about 0.1-s duration, with little scattered energy, to very complex looking signals of a second or more duration. Figure 11 presents a selection of seismograms with simple pulse shapes. A curious thing is observed by comparing these seismograms with the more complex seismograms (e.g., 87 and 57 in Figure 2; 138 in Figure 3; 129 and 130 in Figure 4). Seismograms with simple S-waves generally have low P-wave amplitudes relative to the S-wave, while the seismograms with complex looking S-waves generally have high P-wave amplitudes relative to the S-waves (all the seismograms presented by Tucker and Brune were normalized to the same peak amplitude for plotting purposes; they actually represent a wide range in magnitude).

The obvious explanation for this phenomenon is that it is an effect of radiation pattern [Tucker and Brune, 1977]. Near a node for S-waves there will tend to be an antinode for P-waves (relatively high P-wave amplitudes), whereas S-waves will appear complex because scattered energy will be large relative to the main S-wave energy. On the other hand, near an antinode for S-waves, the P-wave will tend to be small, and the S-wave will appear simple because it will stand out from the smaller scattered

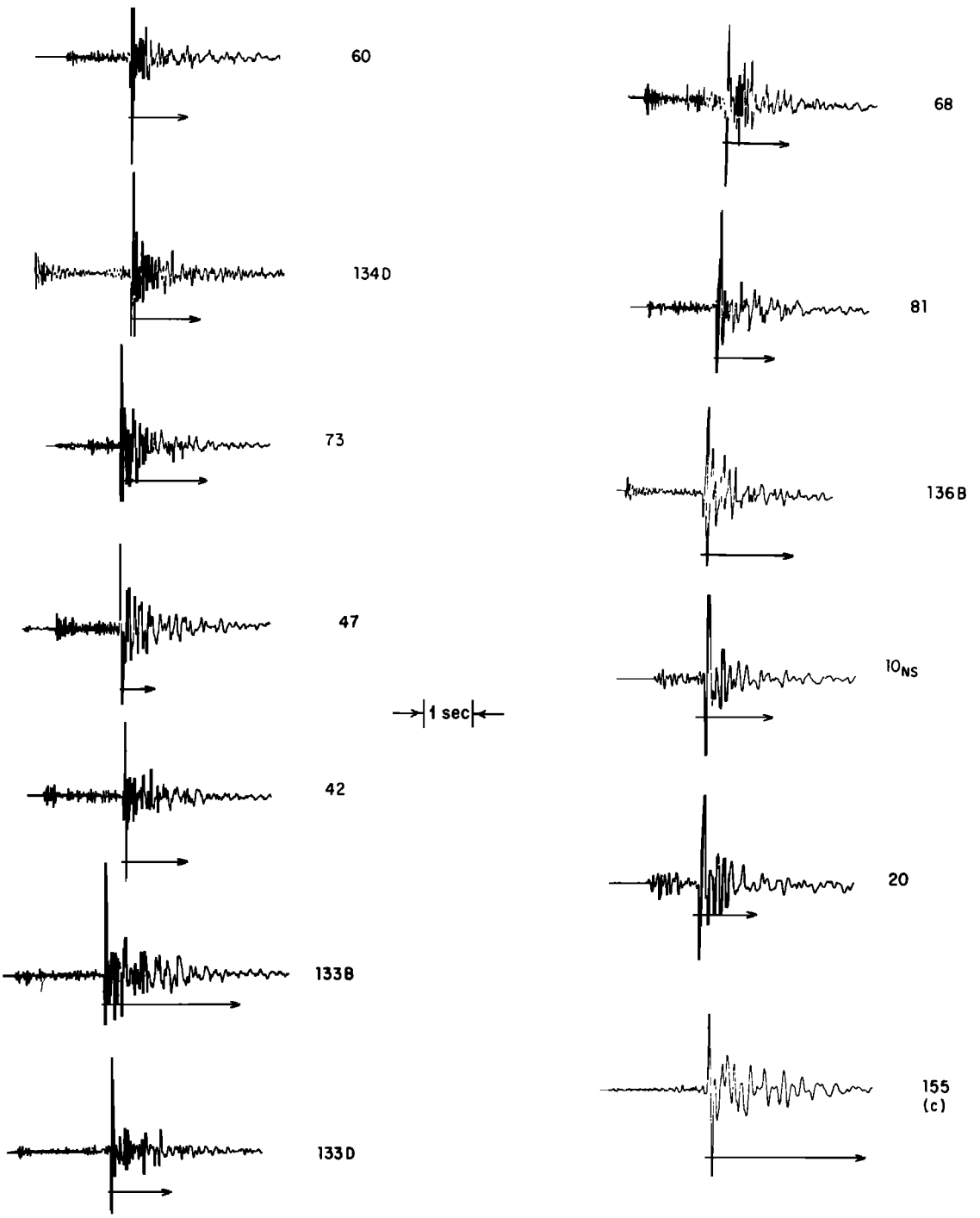

Fig. 11. Aftershocks of the San Fernando earthquake with simple S-waves, suggesting little scattering of energy. Figure 2, events 87 and 57, illustrate more complex seismograms.

energy. If we accept this explanation, we can estimate the amount of scattering by observing the time functions of the simpler events. Figure 12 shows two simple time functions constructed as examples of predicted S-wave pulses when no scattering is present. These are compared with two of the simple observed pulse shapes. The theoretical pulses were diagramatically constructed so as to correspond to a simple smooth spectrum with the same corner frequency as determined experimentally, with a time function similar to the theoretical pulse used by Brune [1970], as seen through a simple velocity transducer of the type used by Tucker and Brune [1977]. For the purposes of determining the approximate amount of scattered energy, it is not important whether or not this pulse is exactly correct; we are interested in the amount of late arriving scattered energy relative to the main pulse. As can be seen from the seismograms in this figure, when the S-pulse is simple, the scattered late arriving energy is quite small

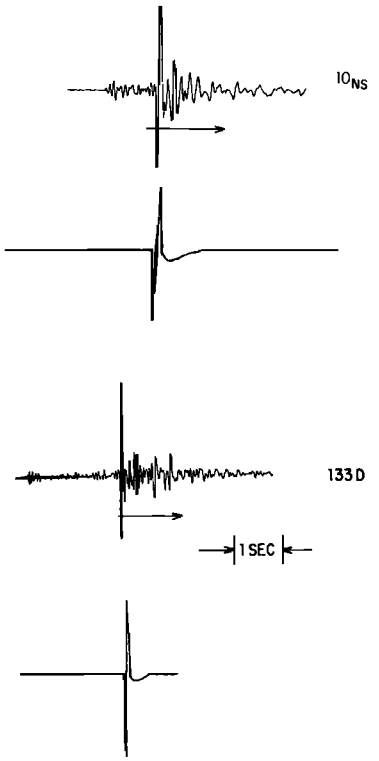

Fig. 12. Comparison of two simple observed records of San Fernando aftershocks and theoretical S-wave pulses diagramatically constructed for the case when no scattering is present.

relative to the main energy, probably not enough to affect the inferred corner frequencies seriously. The effect of scattering could be more serious for the more complex looking seismograms. However, study of the results of Tucker and Brune does not indicate any obvious correlation of stress drop with complexity, suggesting that, as expected, the scattered energy has about the same spectrum as the direct energy. Further evidence of this is the fact that in a number of trials to determine the effect of record length on the shape of the spectrum, Tucker and Brune found very little effect, i.e., adding more or less of the S-wave coda, presumably scattered energy, had little effect on the spectrum shape. We conclude that at least for the San Fernando aftershocks studied by Tucker and Brune, scattering did not seriously affect the observed spectra. Other effects such as variation in source parameters, source complexity, and direction of rupture propagation were probably more important in causing the variations in spectral shape (and inferred stress drop) observed by Tucker and Brune.

References

Archambeau, C. B., General theory of elastodynamic source fields, Rev. Geophys., 6, 241-288, 1968.

Archuleta, R. J., Experimental and numerical three-dimensional simulations of strike-slip earthquakes, Ph.D. Thesis, University of California, San Diego, 1976.

Archuleta, R. J., and J. N. Brune, Surface strong motion associated with a stick-slip event in a foam rubber model of earthquakes, Bull. Seism. Soc. Am., 65, 1059-1071, 1975.

Archuleta, R. J., and G. A. Frazier, Three-dimensional numerical simulations of dynamic faulting in a half-space, Bull. Seism. Soc. Am., 68, 541-572, 1978.

Ben-Menahem, A., Radiation patterns of seismic surface waves from finite moving sources, Bull. Seism. Soc. Am., 51, 401-435, 1961.

Brune, J. N., Tectonic stress and the spectra of seismic shear waves from earthquakes, J. Geophys. Res., 75, 4997-5009, 1970.

Brune, J. N., Correction, J. Geophys. Res., 76, 5002, 1971.

Dahlen, F. A., On the ratio of P-wave to S-wave corner frequencies for shallow earthquake sources, Bull. Seism. Soc. Am., 64, 1159-1180, 1974.

Hartzell, S. H., Interpretation of earthquake strong ground motion and implications for earthquake mechanism, Ph.D. Thesis, University of California, San Diego, 1978.

Hartzell, S. H., and J. N. Brune, Source parameters for the January, 1975, Brawley - Imperial Valley earthquake swarm, Pure Appl. Geophys., 115, 333-355, 1977.

Hartzell, S. H., G. A. Frazier, and J. N. Brune, Earthquake modeling in a homogeneous half-space, Bull. Seism. Soc. Am., 68, 301-316, 1978.

Haskell, N., Total energy and energy spectral density of elastic wave radiation from propagating faults, Bull. Seism. Soc. Am., 54, 1811-1842, 1964.

Johnson, L. R., Green's function for Lamb's problem, Geophys. J. Roy. astr. Soc., 37, 99-131, 1974.

Madariaga, R., Dynamics of an expanding circular fault, Bull. Seism. Soc. Am., 66, 639-666, 1976.

Madariaga, R., Implications of stress-drop models of earthquakes for the inversion of stress drop from seismic observations, Pure Appl. Geophys., 115(112), 301-316, 1977.

Molnar, P., B. E. Tucker, and J. N. Brune, Croner frequencies of P and S waves and models of earthquake sources, Bull. Seism. Soc. Am., 63, 2091-2105, 1973.

Randall, M. J., The spectral theory of seismic sources, Bull. Seism. Soc. Am., 63, 1133-1144, 1973.

Savage, J. C., Relation of corner frequency to fault dimensions, J. Geophys. Res., 77, 3788-3795, 1972.

Savage, J. C., Relation between P- and S-wave corner frequencies in the seismic spectrum, Bull. Seism. Soc. Am., 64, 1621-1627, 1974.

Tucker, B. E., and J. N. Brune, Seismograms, S-wave spectra and source parameters for aftershocks of the San Fernando earthquake of February 9, 1971, special report, Nat. Oceanic and Atmos. Admin., Boulder, Colo., 1973.

Tucker, B. E., and J. N. Brune, Source mechanism and m_b-M_s analysis of aftershocks of the San Fernando earthquake, Geophys. J. Roy. astr. Soc., 49, 371-426, 1977.

(Received March 20, 1978;
revised July 18, 1978;
accepted September 7, 1978.)